

Measurement of the Anisotropic Temperature Relaxation Rate in a Pure Electron Plasma

A. W. Hyatt, C. F. Driscoll, and J. H. Malmberg

Department of Physics, University of California, San Diego, La Jolla, California 92093

(Received 10 September 1987)

The anisotropic temperature relaxation rate is obtained from the measured time evolution of T_{\perp} and T_{\parallel} in a magnetized plasma consisting of only electrons. The velocity-space anisotropy is induced by an essentially one-dimensional compression (or expansion) which changes T_{\parallel} but not T_{\perp} . T_{\perp} and T_{\parallel} are then measured as they relax to a common value. The relaxation rate is obtained as a function of plasma density and temperature. Good agreement with collisional Fokker-Planck theory is found over a range of two decades.

PACS numbers: 52.25.Wz, 52.25.Dg

The collisional scattering in velocity space of a system of charged particles is a fundamental process in plasma physics. A few examples where this process can dominate are the equipartition of energy among the various degrees of freedom in a plasma, the scattering of charged particles into a specific region of velocity space (the loss cone of a magnetic mirror, for instance), and the momentum exchange between electrons and ions (resistivity). A theoretical description of collisional velocity scattering has been the subject of continuing effort over the past fifty years. Small-momentum-transfer collisions are thought to dominate, a view which has led to a Fokker-Planck approximation to the velocity-scattering process.¹⁻⁹ Many important theoretical results have been obtained with this approach. However, there have been only a few direct experimental tests of the theory,^{10,11} and these tests have uncertainties of order unity.

In this paper we describe a simple and direct experiment which measures one specific case of collisional velocity-space transport: the rate of anisotropic temperature relaxation in a magnetized pure electron plasma. The anisotropy is characterized by T_{\perp} and T_{\parallel} , the temperatures perpendicular and parallel to the applied magnetic field. Our experimental apparatus is particularly well suited to create and to measure accurately the relaxation of this anisotropy. We induce the anisotropy by accomplishing an essentially one-dimensional compression (or expansion) of a quiescent plasma which is initially isotropic and Maxwellian in velocity space. T_{\parallel} changes while T_{\perp} is unaffected. We then obtain the relaxation rate from measurements of the time evolution of T_{\perp} and T_{\parallel} as they relax to a new common value. We obtain the rate for various plasma densities and temperatures. Our measured rates span two decades.

Fokker-Planck theories of collisional velocity-space transport have been obtained by many workers in both the nonmagnetized^{3,4,6} and magnetized regimes.^{5,7,8} Ichimaru and Rosenbluth⁷ (IR) calculate the rate of anisotropic temperature relaxation in a weakly magnetized one-component plasma for which the Larmor radius r_L is much larger than the Debye shielding length λ_D , i.e.,

$r_L \gg \lambda_D$. They employ the "dominant-term" approximation,² which neglects all terms that do not contain the Coulomb logarithm factor $\ln \Lambda$ in the rate. Since terms of relative order $1/\ln \Lambda$ are neglected, the theoretical rate is calculated only to that accuracy, which in our plasma is about 10%.

We can adapt the small-magnetic-field calculation of IR to our experimental regime of $r_L \ll \lambda_D$ by using a general result of Montgomery, Joyce, and Turner⁸ (MJT). MJT have shown that, to good approximation, zero- and small-magnetic-field transport theories can be applied in the regime $r_L < \lambda_D$ if the argument of the Coulomb logarithm is changed from $\Lambda = \lambda_D/b$ to $\lambda = r_L/b$, where $b = e^2/T$ is the classical distance of closest approach. This change can be thought of as a decrease in the range over which effective collisions can occur. The effect of the MJT approximation in our experimental regime is to reduce the theoretical rate of IR by approximately 25%.

When we compare our experimental results with the predictions of this theory we find agreement to within approximately 10% over a two-decade range. This is an absolute comparison, since there are no adjustable parameters in either the theory or the experimental measurements.

A simplified schematic of the experimental device, which has been previously described,¹² is shown in Fig. 1. It provides a stable, confined, pure electron plasma.

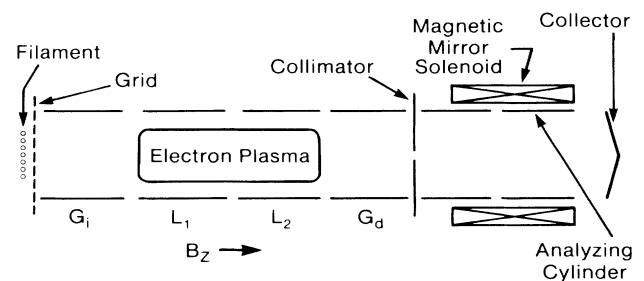


FIG. 1. Simplified schematic of the cylindrical plasma confinement device.

The apparatus consists of several coaxial conducting cylinders in an ultrahigh vacuum (2×10^{-11} Torr) immersed in a uniform axial magnetic field B_z . The magnetic field provides a radial confinement, and negative potentials applied to cylinders G_i and G_d provide axial confinement. The parameters of a typical plasma are density $n = 10^7 \text{ cm}^{-3}$, length $L = 30 \text{ cm}$, temperature $T = 1 \text{ eV}$, and $B_z = 280 \text{ G}$. In this study we have investigated the parameter range $3 \times 10^6 \leq n \leq 3.5 \times 10^7 \text{ cm}^{-3}$ and $0.7 \text{ eV} \leq T \leq 8.5 \text{ eV}$. The confinement properties of this type of pure electron plasma device have been extensively studied.¹²⁻¹⁷ For the purposes of this experiment, the long confinement times (much longer than any other time scale of interest) are important, in that they allow the thermal-evolution experiments to be conducted at constant energy and density. The collisional scattering effects due to background neutrals (densities $\approx 10^6/\text{cm}^3$) are negligible.

We operate the device cyclically: inject; manipulate; dump and measure. To inject the plasma, the inject cylinder G_i is switched to ground, L_1 and L_2 are grounded, and the dump cylinder G_d is set to a negative potential, allowing the formation of a column of electrons extending from the negatively biased filament to G_d . The potential on G_i is then switched negative to capture the electrons in L_1 and L_2 . (It is also possible to capture the electrons in L_1 or L_2 separately.) We allow the injected plasma to equilibrate thermally. We then apply potentials to L_1 or L_2 to compress or expand the plasma axially, which induces the initial velocity-space anisotropy. After allowing the initial anisotropy to evolve for a time t , we dump the plasma axially by grounding G_d . All measurements of the plasma temperatures and density are made at the time of dump. We construct the time evolution of the anisotropy from a number of machine cycles of varying evolution time t . This relies on shot-to-shot reproducibility, which is generally better than 1%.

We obtain the plasma density, $n(r, z)$, by dumping the

plasma axially, then measuring the total charge Q_T which streams through the collimator hole and onto the collector. Repeating this with the collimator at varying radii gives $Q_T(r) = -eA_h \int dz n(r, z)$, where A_h is the area of the hole. We are able to undo this z integral to obtain $n(r, z)$ by assuming that the electrons are in thermal equilibrium along each field line separately, i.e.,

$$n(r, z) = \hat{n}(r) \exp[-e\phi(r, z)/T(r)],$$

where $\phi(r, z)$ is the potential. Given the known boundary conditions for ϕ and the measured quantities $Q_T(r)$ and $T(r)$, we solve Poisson's equation self-consistently for $n(r, z)$ and $\phi(r, z)$. For comparison to theory, we measure $n(r, z)$ after the evolution is completed and then calculate the average density for collisional interactions, as $\bar{n}(r) = \int dz n^2(r, z) / \int dz n(r, z)$.

We obtain the perpendicular temperature, $T_\perp(r, t)$, of the plasma by performing parallel velocity discrimination on the dumped electrons as they pass through a secondary axial magnetic field, B_s , added to B_z .^{18,19} The plasma disassembly process changes the electron parallel energy to a value of E_\parallel , which is dominated by the conversion of space-charge potential to kinetic energy. The electron perpendicular energy, E_\perp , is left unchanged by the disassembly, as a result of the conservation of the electron gyromagnetic moment, $\mu = E_\perp/B$, in the constant field $B = B_z$. After the electron has entered the additional secondary field ($B = B_s + B_z$), conservation of both μ and total energy has caused the electron parallel energy to change further by an amount $\Delta E_\parallel = -(\gamma - 1)E_\perp$, where $\gamma \equiv (B_s + B_z)/B_z$. The electron parallel energy well within the analyzing cylinder is then $E_\parallel - (\gamma - 1)E_\perp$. We measure $Q(V_A, \gamma)$, the charge of all electrons which have sufficient parallel energy to pass through the analyzing cylinder held at potential V_A , as a function of V_A and γ . We assume that the dumped electron energy distribution function is separable (the disassembly process tends to wash out perpendicular and parallel energy correlations), and write $Q(V_A, \gamma)$ as

$$Q(V_A, \gamma) = Q_T \int_0^\infty dE_\perp \int_{[-eV_A + (\gamma - 1)E_\perp]}^\infty dE_\parallel f(E_\parallel) g(E_\perp). \quad (1)$$

The average perpendicular energy of the electrons is then easily obtained as

$$\langle E_\perp \rangle = -e \left. \frac{\partial Q(V_A, \gamma) / \partial \gamma}{\partial Q(V_A, \gamma) / \partial V_A} \right|_{\gamma=1}, \quad (2)$$

which is independent of V_A . If $g(E_\perp)$ is Maxwellian, then $\langle E(r, t) \rangle = T(r, t)$.

Alternatively, we can measure the parallel temperature of the confined plasma by collecting the electrons which are energetic enough to escape past the confinement potential V_d applied to G_d as this potential is slowly made less negative. If the escaped electrons had a distribution of parallel energies $f(E_\parallel) \propto \exp(-E_\parallel/T_{\parallel\epsilon})$

when confined, then the escaping charge will vary initially as

$$[Q(V_d)]^{-1} dQ(V_d) / dV_d \approx -(eT_{\parallel\epsilon})^{-1}. \quad (3)$$

This relation is valid only as long as the plasma potential remains essentially unchanged, i.e., only until about 10^{-4} of the total charge has escaped. Because of this restriction, the measured temperature $T_{\parallel\epsilon}$ is characteristic of the energetic tail of the distribution (hence the subscript " ϵ "), and, furthermore, can be measured only on the axis. However, when we measure both $T_{\parallel\epsilon}$ and $\langle E_\perp \rangle$ for a plasma equilibrium, we typically obtain $T_{\parallel\epsilon} = \langle E_\perp \rangle$

$\equiv T_{\text{eq}}$ to within 5%.

We now describe how the relaxation rates are obtained, using one experimental data set for illustration. All of our rates are obtained from temperatures measured on the axis. In Fig. 2 we show the measured time evolution of $\langle E_{\perp} \rangle$ and $T_{\parallel\epsilon}$. Initially the plasma is captured in cylinder L_2 . It is allowed to evolve to an isotropic temperature $T=1.47$ eV, and to a density profile which is essentially constant over the area of the collimator hole. At $t=0$, we expand the plasma into L_1 by ramping L_1 to ground on a time scale much longer than the axial bounce time yet much shorter than the collision time. The expansion thus preserves the adiabatic bounce invariant $J=\oint v_{\parallel} dz$. Ideally, the result would be a one-dimensional expansion with T_{\parallel} changed by the ratio $[L_2/(L_1+L_2)]^2$, and T_{\perp} unchanged. In practice, the plasma lengths are not exactly equal to the cylinder lengths, and T_{\perp} is slightly changed since the expansion requires some finite fraction of a collision time to complete. This does not materially affect the net result, which is the creation of an anisotropic temperature distribution $T_{\perp} > T_{\parallel}$. We then measure $\langle E_{\perp}(t) \rangle$ and $T_{\parallel\epsilon}(t)$ as they relax towards the common equilibrium value of $T_{\text{eq}}=1.08$ eV.

From the observation that $\langle E_{\perp}(t) \rangle$ and $T_{\parallel\epsilon}(t)$ become constant at large t , we deduce that energy sources or sinks may be neglected during the relaxation, i.e., $\frac{1}{3} T_{\parallel}(t) + \frac{2}{3} T_{\perp}(t) = T_{\text{eq}}$. We thus can write the rate equations of IR as

$$d(T_{\perp} - T_{\text{eq}})/dt = -\nu(T_{\perp} - T_{\text{eq}}), \quad (4a)$$

and similarly

$$d(T_{\parallel} - T_{\text{eq}})/dt = -\nu(T_{\parallel} - T_{\text{eq}}), \quad (4b)$$

where $\nu(n, T_{\perp}, T_{\text{eq}}, B_z)$ is the common relaxation rate. ν

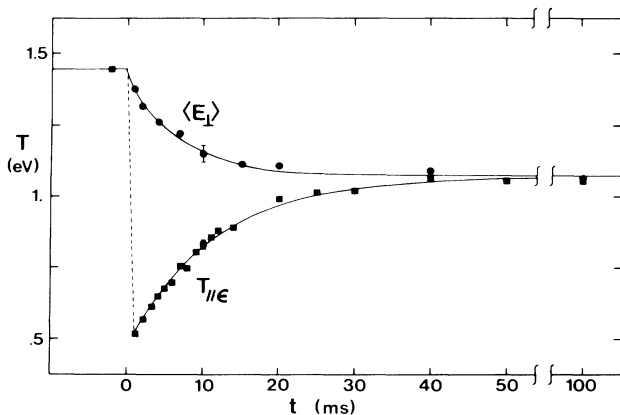


FIG. 2. Data showing the creation and subsequent relaxation to equilibrium of an anisotropic temperature distribution. The expansion which creates the anisotropy begins at $t=0$ and lasts for 1 msec. The solid lines are least-squares fits of the model to the data points.

can be put into the form $\nu = \bar{\nu} h(T_{\perp}/T_{\text{eq}})$, where $\bar{\nu}$ is the relaxation rate in equilibrium, and $h(T_{\perp}/T_{\text{eq}})$ is a correction factor [$h(1)=1$] for the degree of anisotropy.⁷ In our experiments the correction is always small. The theory of IR predicts

$$\bar{\nu} = \frac{8}{5} (\pi/m_e)^{1/2} \bar{n} e^4 \ln \Lambda / T_{\text{eq}}^{3/2}. \quad (5)$$

For comparison, we note that $\bar{\nu} = \frac{6}{5} \nu_{\text{eq}}$, where

$$\nu_{\text{eq}} = 4(\pi/m_e)^{1/2} \bar{n} e^4 \ln \Lambda / 3 T_{\text{eq}}^{3/2}$$

is the Spitzer rate of energy equipartition³ between an isotropic Maxwellian electron plasma and a Maxwellian distribution of test electrons. For comparison with experimental results, we modify $\ln \Lambda$ in Eq. (5) as per MJT.

Although Eqs. (4a) and (4b) were derived only for Maxwellian distributions, we substitute $\langle E_{\perp} \rangle$ for T_{\perp} and $T_{\parallel\epsilon}$ for T_{\parallel} . We make a least-squares fit to the $\langle E_{\perp}(t) \rangle$ and $T_{\parallel\epsilon}(t)$ data independently using the general solution to Eqs. (4a) and (4b) as the model, and we display the results as the two solid lines in Fig. 2. The $\langle E_{\perp} \rangle$ data yield a rate $\bar{\nu}_{\perp} = 121 \text{ sec}^{-1}$, while the $T_{\parallel\epsilon}$ data yield a rate $\nu_{\parallel} = 79 \text{ sec}^{-1}$, which is significantly lower. This can be understood from the energy dependence of the two-charged-particle (Coulomb) cross section, wherein the cross section decreases as (energy)⁻². Since ν_{\parallel} is some measure of the collisionality of the energetic tail of the parallel distribution, it is not surprising that ν_{\parallel} is less than $\bar{\nu}_{\perp}$, which is measured over the entire perpendicular distribution. Since we believe that $\langle E_{\perp} \rangle = T_{\perp}$ is a much better approximation than $T_{\parallel\epsilon} = T_{\parallel}$ during the relaxation, we obtain our $\bar{\nu}$ results from $\langle E_{\perp} \rangle$ evolution only.

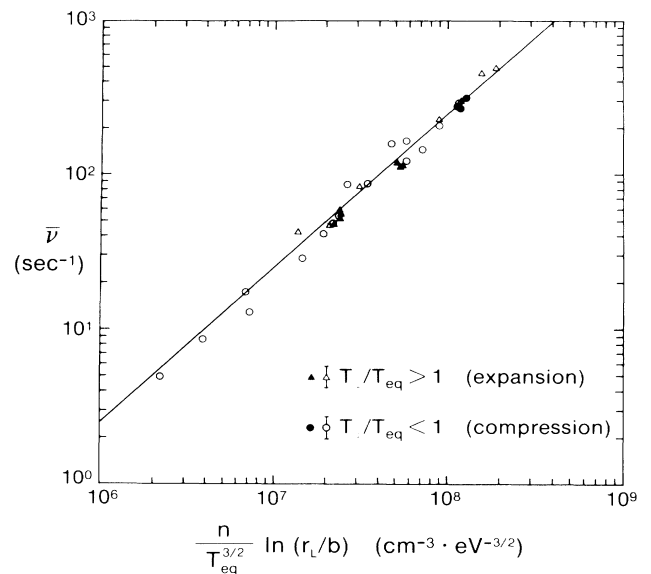


FIG. 3. Experimentally measured relaxation rates $\bar{\nu}$ for various electron plasma densities and temperatures. The solid line is the absolute prediction of theory. Solid symbols have statistical errors of $\approx 3\%$, open symbols $\approx 15\%$. B_z is 281 G.

In Fig. 3 we display the comparison between our measured rates and the theory IR as modified by MJT. On the abscissa is the expected parameter scaling and on the ordinate is the relaxation rate $\bar{\nu}$. Most of the data points have error bars of $\approx 15\%$. A recently adopted noise-reduction technique has allowed the measurement of a few points with $\approx 3\%$ error bars; these are displayed as solid symbols in Fig. 3. B_z was held fixed at 281 G for all points. The solid line is the prediction of theory and there are no adjustable parameters. A weighted least-squares fit to the measured rates with use of $\bar{\nu}(\text{fit}) = \alpha \bar{\nu}(\text{theory})$ gives $\alpha \approx 0.95$. This would give a line about 5% below the theory line in Fig. 3. Since the theory is calculated to an accuracy of approximately 10%, we regard the measurements and the theory as being in very good agreement.

We do not believe that collective instabilities have significantly contributed to our measured rates, since the agreement with theory is so good. An instability driven by the temperature anisotropy could contribute to isotropization. However, linear stability theory²⁰ predicts suppression of the Weibel or Weibel-type instability in our parameter regime. Furthermore, the agreement of measured rates from both the $T_{\perp}/T_{\parallel} < 1$ and $T_{\perp}/T_{\parallel} > 1$ anisotropy data argues against significant isotropization due to instability, since typically only one type of anisotropy may lead to growth.

We wish to stress the point that our quoted errors represent only statistical measurement errors. The possibility of systematic errors also exists. We consider the density and temperature calibrations to be $\pm 5\%$. One possible source of systematic error is the assumption that both velocity distributions remain Maxwellian during the evolution to equilibrium, i.e., $\langle E_{\perp} \rangle$ is substituted for T_{\perp} in Eq. (4a). There may be other sources of error. We believe that our aggregate systematic errors may be on the order of 10%.

In summary, we have experimentally obtained the anisotropic temperature relaxation rate in a magnetized electron plasma. The measured rate agrees over 2 orders of magnitude with a theoretical calculation of that rate in a magnetized plasma based on a collisional Fokker-Planck-type theory of Ichimaru and Rosenbluth as modified by Montgomery, Joyce, and Turner.

The authors wish to thank Professor T. M. O'Neil for helpful theoretical discussions. This work was supported

by National Science Foundation Grant No. PHY83-06077 and U.S. Office of Naval Research Contract No. N00014-82-K-0621.

-
- ¹L. Landau, *Phys. Z. Sowjetunion* **10**, 154 (1936).
²S. Chandrasekhar, *Astrophys. J.* **97**, 255, 263 (1943), and *Principles of Stellar Dynamics* (Univ. of Chicago Press, Chicago, 1942).
³P. S. Cohen, L. Spitzer, and P. McR. Routly, *Phys. Rev.* **80**, 230 (1950); L. Spitzer, *Physics of Fully Ionized Gases* (Interscience, New York, 1956).
⁴M. N. Rosenbluth, W. M. MacDonald, and D. L. Judd, *Phys. Rev.* **107**, 1 (1957).
⁵N. Rostoker and M. N. Rosenbluth, *Phys. Fluids* **3**, 1 (1960).
⁶W. B. Thompson and J. Hubbard, *Rev. Mod. Phys.* **32**, 714 (1960).
⁷S. Ichimaru and M. N. Rosenbluth, *Phys. Fluids* **13**, 2778 (1970).
⁸D. Montgomery, G. Joyce, and L. Turner, *Phys. Fluids* **17**, 954, 2201 (1974).
⁹M. Matsuda, *Phys. Fluids* **26**, 1247 (1983).
¹⁰A short list of experimental results of fast-ion slowing in magnetized plasma can be found in R. J. Burke and R. F. Post, *Phys. Fluids* **17**, 1422 (1974).
¹¹A short list of velocity-space transport experimental results in mirror machines can be found in J. R. Hiskes and A. H. Futch, *Nucl. Fusion* **14**, 116 (1974).
¹²C. F. Driscoll, K. S. Fine, and J. H. Malmberg, *Phys. Fluids* **29**, 2015 (1986).
¹³J. H. Malmberg and J. S. deGrassie, *Phys. Rev. Lett.* **35**, 577 (1975).
¹⁴J. S. deGrassie and J. H. Malmberg, *Phys. Fluids* **23**, 63 (1980).
¹⁵M. H. Douglas and T. M. O'Neil, *Phys. Fluids* **21**, 920 (1978).
¹⁶J. H. Malmberg and C. F. Driscoll, *Phys. Rev. Lett.* **44**, 654 (1980).
¹⁷C. F. Driscoll and J. H. Malmberg, *Phys. Rev. Lett.* **50**, 167 (1983).
¹⁸T. Hsu and J. L. Hirschfield, *Rev. Sci. Instrum.* **47**, 236 (1976).
¹⁹J. S. deGrassie, Ph.D. dissertation, University of California, San Diego, 1977 (unpublished), pp. 81–86.
²⁰R. C. Davidson, in *Handbook of Plasma Physics*, edited by M. N. Rosenbluth and R. Z. Sagdeev (North-Holland, Amsterdam, 1983), Vol. 1, Chap. 3.3.